Predicting current and future global distributions of whale sharks

ANA M. M. SEQUEIRA*, CAMILLE MELLIN*†, DAMIEN A. FORDHAM*, MARK G. MEEKAN‡ and COREY J. A. BRADSHAW*§

*The Environment Institute and School of Earth and Environmental Sciences, The University of Adelaide, South Australia 5005, Australia, †Australian Institute of Marine Science, PMB No. 3, Townsville MC, Townsville, Queensland 4810, Australia, ‡Australian Institute of Marine Science, UWA Oceans Institute (MO96), 35 Stirling Hwy, Crawley, Western Australia 6009, Australia, §South Australian Research and Development Institute, P.O. Box 120, Henley Beach, South Australia 5022, Australia

Abstract

The *Vulnerable* (IUCN) whale shark spans warm and temperate waters around the globe. However, their present-day and possible future global distribution has never been predicted. Using 30 years (1980–2010) of whale shark observations recorded by tuna purse-seiners fishing in the Atlantic, Indian and Pacific Oceans, we applied generalized linear mixed-effects models to test the hypothesis that similar environmental covariates predict whale shark occurrence in all major ocean basins. We derived global predictors from satellite images for chlorophyll *a* and sea surface temperature, and bathymetric charts for depth, bottom slope and distance to shore. We randomly generated pseudo-absences within the area covered by the fisheries, and included fishing effort as an offset to account for potential sampling bias. We predicted sea surface temperatures for 2070 using an ensemble of five global circulation models under a no climate-policy reference scenario, and used these to predict changes in distribution. The full model (excluding standard deviation of sea surface temperature) had the highest relative statistical support ($wAIC_c = 0.99$) and explained ca. 60% of the deviance. Habitat suitability was mainly driven by spatial variation in bathymetry and sea surface temperature among oceans, although these effects differed slightly among oceans. Predicted changes in sea surface temperature resulted in a slight shift of suitable habitat towards the poles in both the Atlantic and Indian Oceans (ca. 5°N and 3–8°S, respectively) accompanied by an overall range contraction (2.5–7.4% and 1.1–6.3%, respectively). Predicted changes in the Pacific Ocean were small. Assuming that whale shark environmental requirements and human disturbances (i.e. no stabilization of greenhouse gas emissions) remain similar, we show that warming sea surface temperatures might promote a net retreat from current aggregation areas and an overall redistribution of the species.

Keywords: climate change, conservation, global ocean, global warming, remote sensing, *Rhincodon typus*, sea surface temperature, species distribution models, tuna purse-seine fisheries

Received 18 November 2012; revised version received 27 June 2013 and accepted 20 July 2013

Introduction

Changes in climate, such as warming temperatures, are expected to alter the current distribution of species (Thomas *et al.*, 2004; Parmesan, 2006; Wernberg *et al.*, 2011). Despite a bias of studies towards terrestrial habitats (Richardson & Poloczanska, 2008), there is mounting evidence for distributional shifts in the marine environment (e.g., Edwards & Richardson, 2004), which generally result in changes in pole-ward latitudinal (e.g., Perry *et al.*, 2005) or depth (e.g., Dulvy *et al.*, 2008) ranges. These shifts have been reported in species as divergent as plankton (Beaugrand *et al.*, 2009), demersal fish (Perry *et al.*, 2005; Dulvy *et al.*, 2008) and macroalgae (Wernberg *et al.*, 2011).

Correspondence: Ana M. M. Sequeira, tel. +61 0 8 6488 2219, fax +61 0 8 8313 4347, e-mail: ana.sequeira@uwa.edu.au

However, assessing how much the distribution of species will be affected by climate change implies that the current distribution of the species is adequately identified.

A species' distribution and its habitat requirements can be estimated by modelling information on occurrence together with environmental correlates (Guisan & Zimmermann, 2000). Species distribution models (also known as ecological niche models and bioclimatic envelope models) have now been used for many marine species including reef fish (Mellin *et al.*, 2010), mammals (e.g., Praca & Gannier, 2007) and sharks (McKinney *et al.*, 2012; Sequeira *et al.*, 2012). However, applying such models to highly migratory marine species is particularly challenging due to poor detection (Elith & Leathwick, 2009), lack of recorded occurrences in the open ocean (McKinney *et al.*, 2012), and the large geographical range of the species under consideration (Sequeira *et al.*, 2012, 2013a).

The whale shark (*Rhincodon typus* Smith 1828), the largest of all fish, has a circumglobal range between 30°N and 35°S (Compagno, 2001). This range was defined based on occasional occurrences and on the range of temperatures where the species is expected to occur: tropical/warm temperate. Whale sharks occur regularly at the ocean surface within a narrow range of sea surface temperatures (Sequeira *et al.*, 2012), possibly to assist thermoregulation (Thums *et al.*, 2012). Like most marine organisms (Tittensor *et al.*, 2010), and especially ectotherms, ambient temperatures directly influence metabolic processes. Therefore, changes in climate are likely to affect whale shark distribution or abundance as they adapt to new temperature regimes and changing prey distributions (Gutierrez *et al.*, 2008).

Whale sharks are regularly recorded in specific locations near shore where they occur seasonally (Sequeira *et al.*, 2013b), and to where they attract substantial tourism interest due to their innocuous behaviour and large size (e.g., Cárdenas-Torres *et al.*, 2007). Concerns about population declines driven by human activities such as illegal fishing (Riley *et al.*, 2009), habitat disturbance due to tourism (Heyman *et al.*, 2010) or shipping (Speed *et al.*, 2008), have prompted a research focus on documenting migratory pathways to determine whether partial-range protection is sufficient to ensure persistence at current aggregation locations (Rowat, 2007; Bradshaw *et al.*, 2008; Sequeira *et al.*, 2013b). In addition to these direct threats, climate change might already be affecting whale sharks. However, the species' high mobility and the lack of extensive occurrence data mean that teasing apart spatial and temporal patterns is problematic (Sequeira *et al.*, 2013a). Thus, determining whether departures from current distributional limits (Turnbull & Randell, 2006; Rodrigues *et al.*, 2012) or temporal patterns in relative abundance (e.g., Bradshaw *et al.*, 2008) are linked to changing temperatures (e.g., Sleeman *et al.*, 2007) is equally difficult.

Statistical tools can facilitate inference in this regard. For example, known occurrences can be used to define the current distribution of a species, and future distributions can be projected by coupling climate forecasts derived from global circulation models (e.g., Araújo *et al.*, 2005). Despite the known limitations of these statistical approaches (Elith & Leathwick, 2009), confidence in their outcomes can be improved by addressing potential biases in occurrence data (Phillips *et al.*, 2009; Barbet-Massin *et al.*, 2012) and better understanding how abiotic conditions and dispersal potential have influenced species' geographic distributions over time (Barve *et al.*, 2011). Another important way to improve predictions derived from global circulation models, especially from a conservation perspective, is by downscaling the coarse resolution (2.5–5-° grid cells)

of the forecasts (Hannah *et al.*, 2002), and generating multi-model climate projections (Fordham *et al.*, 2013b). Estimates of range shifts under climate change can be further strengthened by coupling correlative distribution models to ecological processes, when adequate data are available to determine conceptual structural relationships (Fordham *et al.*, 2013a).

For the first time, we used a global dataset of pelagic whale shark sightings derived from tuna purse-seine fisheries operating in the Atlantic, Indian and Pacific Oceans to: (i) predict the spatial distribution of whale shark habitat suitability across three ocean basins; and (ii) extend our projections to a future scenario of ocean warming based on a no climate-policy reference (i.e. no stabilization of greenhouse gas emissions). Following our previous work where we derived ocean-basin scale predictions for whale shark distribution and temporal trends (Sequeira *et al.*, 2012, 2013a,b), our overarching aim here was to derive realistic predictions of the species current geographical (circumglobal) range and provide a modelling tool for exploring the species' future distribution under anticipated climate change.

Materials and methods

Data

We obtained whale shark presence data (henceforth, 'sightings') from the logbooks of tuna purse-seine fisheries. While impounding tuna schools with a purse-seine net, these tuna-targeting fisheries often also surround (and subsequently release) whale sharks (Chassot *et al.*, 2009). The date and location (0.01° precision) of these whale shark-associated net sets were recorded in the logbooks, and data were provided by the Institut de Recherche pour le Développement (France) and Indian Ocean Tuna Commission for the Atlantic and Indian Oceans, and by the Secretariat of the Pacific Community for the western Pacific Ocean (Table 1 and Fig. 1).

The full dataset spans the three major oceans with a maximum temporal coverage of 31 years for the Atlantic Ocean (1980–2010) from 21°N to 15°S and 34°W to 14°E, 17 years (1991–2007) in the Indian Ocean from 30°N to 30°S and 35 to 100°E and 11 years (2000–2010) in the western Pacific Ocean from 15°N to 15°S and 130°E to 150°W (Table 1 and Fig. 1). Data included (i) the number of whale shark sightings (Table 1 and Fig. 1a) and location (longitude and latitude at 0.01°precision); and (ii) fishing effort (days; Fig. 1b) per month and per year pooled for each 5° of longitude by 5° of latitude (5-° grid cell) both in the Indian (6618 records) and western Pacific (2272 records) Oceans, and for both 5-° and 1-° grid cells in the Atlantic Ocean (maximum of 18 277 records), and were therefore comparable. No information was made available on vessel or trip units for any ocean, or on the specific timing of sightings. The data from the western Pacific Ocean, even though representative of total tuna purse-seine fisheries in the area (P. Williams pers. comm.), were incomplete

Table 1 Number of whale shark sightings in each ocean per decade as recorded by tuna purse-seine fisheries (source: Indian Ocean Tuna Commission and the Institut de Recherche pour le Développement, France for the Atlantic [Atl] and Indian [Ind], and Secretariat of the Pacific Community for the western Pacific [Pac]). See also Fig. 1. Numbers of sightings are split by quarters of the year: January–March, April–June, July–September and October–December). Boldface indicates data used to fit models. Numbers for the western Pacific are derived from observer data only

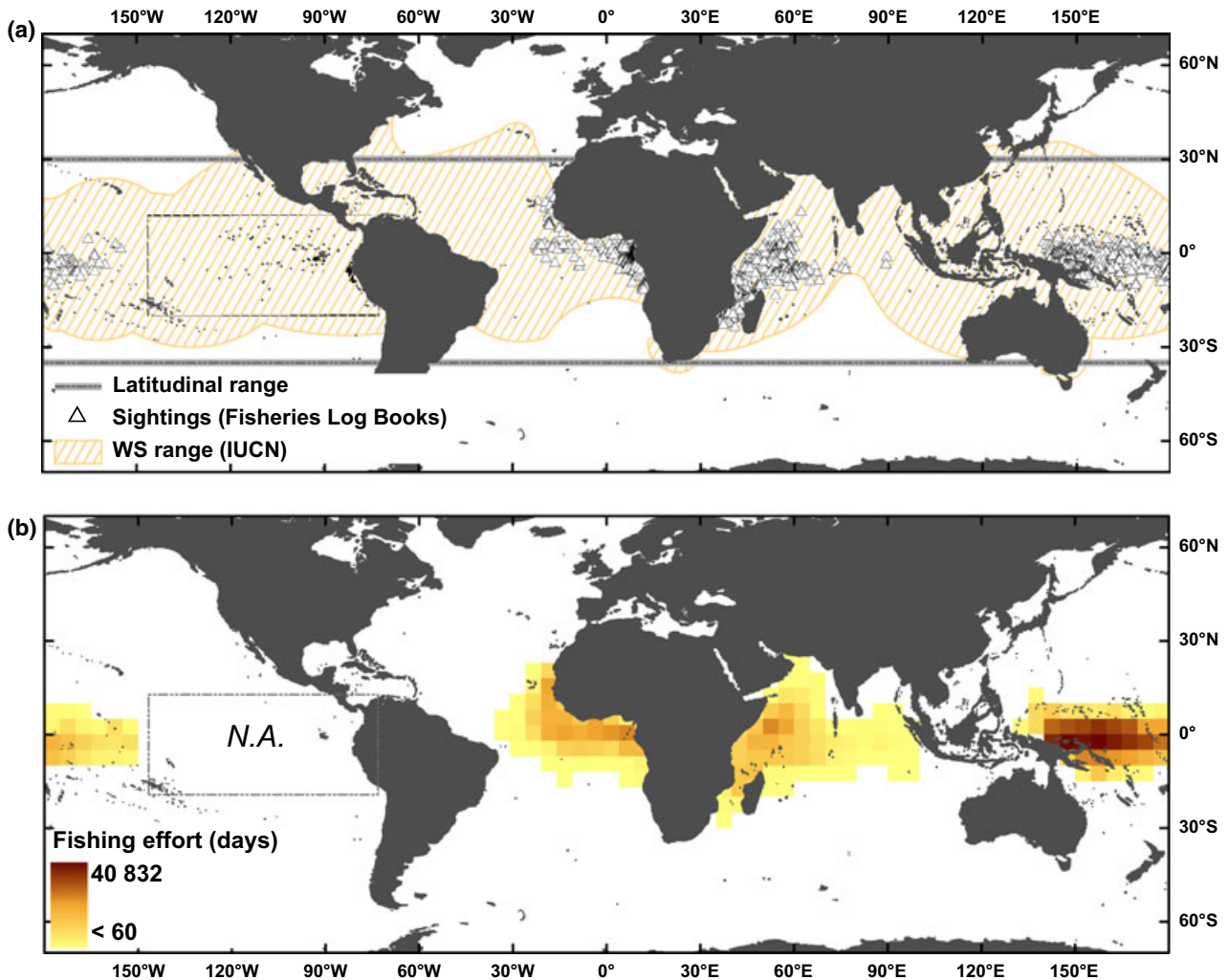|	January–March			April–June			July–September			October–December			Totals		
Period	Atl	Ind	Pac	Atl	Ind	Pac	Atl	Ind	Pac	Atl	Ind	Pac	Atl	Ind	Pac
1980–1989	2	–	–	405	–	–	**310**	–	–	17	–	–	734	–	–
1990–1999	2	92	–	518	**599**	–	**543**	40	–	12	36	–	1075	767	–
2000–2010	3	23*	**314**	147	**212***	167	**300**	27*	189	38	155*	185	488	417*	855
Totals	7	115	**314**	1070	**811**	167	**1153**	67	189	67	191	185	2297	1184	855

*Indian Ocean data are for the period 2000–2007.

Fig. 1 Fisheries data derived from tuna purse-seine fishery logbooks in the Atlantic, Indian and western Pacific Oceans. (a) Sightings from 1980 to 2010: 4336 whale sharks records, with 53% of sightings in the Atlantic, 27% in the Indian from 1991 to 2007, and 20% in the western Pacific from 2000 to 2010. Shaded area shows whale shark geographical range (*WS range*) defined by the International Union for Conservation of Nature, and thick, grey lines mark current latitudinal range (Compagno, 2001). (b) Tuna purse-seine fishing effort for the Atlantic, Indian and western Pacific Oceans (the common resolution of 5 ° was used for easier comparison). Data from the eastern Pacific (dots within inset) consisted of locations without information on year or season of sighting (*NA* in Map b) and were thus not included in the analysis.

because access was not granted from all fleets registered with the Secretariat of the Pacific Community.

Because whale shark numbers fluctuate seasonally (Table 1), with peaks of occurrence in different seasons (referred to as 'quarters' of the year) in each ocean and in a spatially inconsistent manner (Sequeira *et al.*, 2013a), we first defined maximum suitable whale shark habitat based on season in which the highest number of sharks was recorded for each ocean. A seasonal maximum of 314 whale sharks was recorded in the western Pacific between January and March, 811 in the Indian Ocean between April and June, and 1153 between July and September in the Atlantic Ocean (Table 1).

Binary data (presence and absence) are required for binomial estimation in regression models; therefore, we generated pseudo-absences (10 : 1 pseudo-absence:presence ratio, following Barbet-Massin *et al.*, 2012) based on a random spatial distribution within the area covered by the fisheries (excluding presence locations). We used the srswor function (*simple random sampling without replacement*) from the {sampling} package in the *R* programming language (R Development Core Team, 2012), and generated random pseudo-absences among non-presence grid cells in each ocean within the same season for which the presences were being considered. To assess the influence of the chosen pseudo-absences, we generated each set 10 times prior to their inclusion in the spatial GLMM (described below).

We collated an environmental dataset at a 9 km resolution composed of six physical variables: (i) distance to shore (*shore*; km) calculated with the *Near* tool in ArcGIS 9.3.1™ (Redlands, CA, USA) using a world equidistant cylindrical coordinate system; (ii) mean depth (*depth*; m); and (iii) slope (*slope*; °) derived from the one-minute grid of the General Bathymetry Chart of the Oceans (GeBCO, 2003); (iv) mean; and (v) standard deviation of sea surface temperature (*SST* and *SSTsd*; °C) derived from daytime measures from the Advanced Very High Resolution Radiometer (AVHRR) PathFinder version 5.0 NOAA, Washington, DC, USA; and (vi) mean concentration of chlorophyll *a* (*Chl a*; mg m^{-3}) (an index of primary productivity) derived from the Sea-viewing Wide Field-of-view Sensor (SeaWiFS; NASA, Washington, DC, USA). We calculated mean sea surface temperature and its standard deviation and mean chlorophyll *a* based on weekly satellite measures available within the total period covered by the fisheries in each ocean using ArcToolBox functions from ArcGIS 9.3.1™ automated with Python scripts. We also included quadratic terms for *depth* and *SST* as predictors in the models, as detailed below. We assessed the monotonic relationship between predictors with the pairs.panels function in the package {psych} in *R* using the Spearman's rank correlation (ρ).

The environmental dataset for each ocean matched the ocean-specific season of maximum whale shark abundance. Areas where environmental predictors were not available (e.g., due to cloud cover) were excluded from the analysis (and are shown in white in the resulting prediction maps).

Generalized linear mixed-effects models

We applied generalized linear mixed-effects models (GLMM) with a binomial error distribution and a logit link function to the full, three-ocean dataset. To account for spatial bias in sampling effort without reducing the spatial resolution of the dataset, we included this variable as an offset, and used the highest resolution available in each ocean. The mixed-effects models included several possible combinations of the fixed effects (i.e. environmental predictors – Table 2) as well as a spatial random effect that represents unobserved random variation within each 1-° grid cell. Including this random effect reduced the spatial autocorrelation observed in the residuals (Sequeira *et al.*, 2013a). To stabilize parameter estimation within the *lmer* function, we standardized the explanatory variables by centring *depth* and *SST*, and log-transforming mean *Chla*, *shore*, *slope* and also *effort*. We also included the interaction terms *ocean × depth*, *ocean × slope* and

Table 2 Summary of generalized linear mixed-effects models relating probability of whale shark occurrence to ocean properties in the Atlantic, Indian and western Pacific during the season of peak occurrences for each ocean. Slope, distance to shore (shore), depth and its quadratic term referred to together as physical variables (Phys); mean sea surface temperature (SST; mean weekly values within the seasons covered in each ocean at a 9-km grid resolution), its quadratic term (SST^2) and standard deviation altogether referred to as 'SST variables' (SST$_{all}$). Average chlorophyll *a* is represented as Chla (mean weekly values within the seasons covered in each ocean at a 9-km grid resolution). Shown for each model are biased-corrected model probabilities based on weights of Akaike's information criterion corrected for small sample sizes (wAICc, only >0.0001 shown), percentage of deviance explained (%De), 10-fold cross validation error (CV error) and kappa statistics. Note: All models included an offset term for effort and a spatial random effect (1-° grid cell). An interaction term between ocean and depth, slope or SST was also included whenever these predictors were present. The GLMM (with a logit link function) can be expressed as: logit ($Presence$) = $\alpha + _i + \gamma_i Z_i + \epsilon_i + \log(fishing effort)$, where $Presence$ is the expected mean probability of sightings occurrence. X and Z represent the fixed and random covariates used in the models: the environmental predictors and the spatial grid respectively. β and γ represent the coefficients associated with the fixed and random effects, respectively, and α is the intercept. The log of fishing effort was included as an offset. The index i corresponds to the number of observations among grid-cells

Model	wAIC$_c$	%De	CVerror	kappa
Phys + SST + SST^2	0.99	57.9	0.09	0.64 ± 0.03
Phys + SST$_{all}$	–	57.8	0.09	0.64 ± 0.03
Phys + Chla	–	57.3	0.09	0.64 ± 0.03
Phys	–	56.9	0.09	0.59 ± 0.03
depth + depth^2	–	56.8	0.12	0.58 ± 0.03
SST + SST^2	–	56.5	0.09	0.57 ± 0.03
SST + SST^2 + Chla	–	56.5	0.09	0.55 ± 0.04
SST$_{all}$	–	56.5	0.09	0.54 ± 0.04
depth	–	55.9	0.09	0.22 ± 0.04
slope	–	55.9	0.09	0.30 ± 0.04
Chla	–	50.8	0.11	0.33 ± 0.03
Shore	–	48.6	0.09	0.33 ± 0.03

ocean × SST, to test the hypothesis that these predictors had similar predictive power in every ocean. To account for non-linear dependencies of occurrence probability with both sea surface temperature (whale sharks mostly occur within a specific range of temperatures; Sequeira *et al.*, 2012) and depth (whale shark are commonly seen near shore, so possibly within specific depth ranges), we included the quadratic terms for depth and mean sea surface temperature through a second-order polynomial function using the *poly* in the {stats} package in R.

We used Akaike's information criterion corrected for small sample sizes (AIC$_c$) to provide an index of Kullback-Leibler (K-L) information loss that we used to assign relative strengths of evidence to the different competing models (Burnham & Anderson, 2004) and the corresponding weights (*w*AIC$_c$) to compare model probabilities and allow for multi-model inference (instead of inference based only on the top-ranked model). We used percentage of deviance explained (%De) to quantify goodness-of-fit, Cohen's Kappa statistic (κ) to assess the model's predictive power (Cohen, 1960), and calculated mean prediction error for the model with highest support using a 10-fold cross-validation (Davison & Hinkley, 1997).

Global projection

We compiled a worldwide environmental dataset as described above and including the same predictors. Here, we used seasonal averages for sea surface temperature and chlorophyll *a* for the last decade (2000–2012) by using data derived from the Moderate Imaging Spectroradiometer (MODIS) Aqua available online (seasonal climatology maps; http://oceancolor.gsfc.nasa.gov/cgi/l3). After fitting the GLMM with the tuna purse-seine data and running predictions for the entire area covered by the fisheries, we used a model-averaging approach (based on *w*AIC$_c$) to project habitat suitability by including the worldwide dataset under current (2000–2012) conditions. As a qualitative validation, we overlaid the currently known locations for whale shark seasonal occurrence (as compiled in Sequeira *et al.*, 2013b) onto these global habitat suitability maps.

Climate change projections

Using the freeware package MAGICC/SCENGEN5.3 (Model for the Assessment of Greenhouse-gas Induced Climate Change – a regional climate SCENario GENerator) (www.cgd.ucar.edu/cas/wigley/magicc/) (Fordham *et al.*, 2012), we generated monthly forecasts of expected change in sea surface temperature in 2070 (relative to 1995) under a no climate-policy reference scenario (no stabilization of greenhouse gas emissions) (cf. MiniCAM Ref. in Clarke *et al.*, 2007). We generated climate change forecasts using five atmospheric-ocean global circulation models (GCM): CCSM-3, MRI-CGCM2.3.2, ECHAM5/MPI-OM, MIROC3.2 (hires) and UKMO-HadCM3 (terminology follows CMIP3 Multi-Model Dataset Archive naming convention; www-pcmdi.llnl.gov/ipcc/about_ipcc. php). These were chosen based on their skill in predicting global sea surface temperatures for the baseline period 1981–2000

(Fordham *et al.*, 2011), using six alternative skill rankings: model bias (i.e. the difference between model and observed spatial means averaged over a user-specified area), pattern correlation, standard and centred root mean-square error and comparison indices devised by Reichler & Kim (2008) and Taylor (2001). We ranked the GCMs according to each statistic and calculated the seasonal and annual cumulative rank (for specific model rankings see Fordham *et al.*, 2013b), and used bilinear interpolation of the GCM data (2.5-° grid cells to a finer resolution of 0.5-° longitude/latitude) to reduce discontinuities in the perturbed climate at the GCM grid-box boundaries (Fordham *et al.*, 2011). We calculated an average change expected per grid cell across months for each season defined here as each quarter of the year (i.e. January–March, April–June, July–September and October–December), and then downscaled the multi-model climate average anomalies using the 'change factor' empirical method. With this method, the low-resolution climate anomaly is added directly to a high-resolution (9-km grid cells) observed sea surface temperature baseline centred on or around 1990 (Fordham *et al.*, 2012). We used these forecasts of sea surface temperature to generate predictions of worldwide whale shark habitat suitability using our species distribution models. We considered the range of predictor values used to fit the model, and masked areas where model predictions occurred outside the environmental space used for the original model fit.

Results

Spatial patterns of occurrence and sampling effort

Whale shark sightings in the Atlantic and Pacific Oceans occurred mostly where sampling effort was highest (Fig. 1), whereas most records in the Indian Ocean fell within the Mozambique Channel, which had lower sampling effort than in the Indian central-west area (Fig. 1b). There was generally higher effort in the Pacific Ocean (Fig. 1b; >40 000 fishing days in some 5-° grid cells), even though the Pacific time series covered only the last decade (i.e. only one-third of the duration of the Atlantic Ocean dataset; Table 1). Within the area covered by the fisheries, mean depth in sighting locations was similar in all three oceans (ca. 3800 m; Fig. S1) but the Pacific bathymetric range was wider and average distances to shore were slightly shorter (ca. 265 km). In the Indian Ocean average distance to shore was greater (ca. 435 km). Sea surface temperature varied among the three oceans (Fig. S1) with cooler temperatures in the Atlantic ranging from 19.4 to 28.3 °C (± 0.31–7.2; July–September), between 25.2 and 31.2 °C (± 0.39–2.57, April–June) in the Indian, and between 26.7 and 30.1 °C (± 0.19–1.36; January–March) in the western Pacific, with the latter having the lowest standard deviation. Chlorophyll *a* values averaged 0.75, 0.18 and 0.11 mg m^{-3} in the Atlantic, Indian and Pacific, respectively.

Habitat suitability prediction

The percentage of deviance explained was highest (58%) for the model including all physical and temperature variables (except standard deviation for sea surface temperature), a spatial random effect (1-° grid cell) and an offset for effort (Table 2). Statistical support ($wAIC_c$) was highest for the same model (0.99; Table 2). As a result of the interaction terms (*SST*, *slope* and *depth* interactions with *ocean*) within the model with the highest statistical support, we found evidence for a different effect of sea surface temperature and depth in each ocean, with both predictors affecting whale shark occurrence in the Atlantic, only sea surface temperature in the Indian, and only depth in the Pacific Ocean.

The resulting GLMM prediction maps (Fig. 2) show suitable habitat in different areas in the Atlantic from July to September, with higher suitability (>0.8) around Gabon, Congo and Equatorial Guinea. The model also predicted high suitability (>0.6) around Côte d'Ivoire, Ghana and Bénin, Cape Verde and Mauritania. In the Indian Ocean, the area around the Mozambique Channel and close to shore in the south-eastern side of the African continent had the highest suitability (ca. 0.3) during the months of April to June. In the western Pacific, the central portion of the total area covered by the fisheries had the highest suitability during the first quarter of the year, but predicted suitability there was the lowest of all three oceans examined (ca. 0.1, equal to prevalence used in the models, i.e. ratio of presences/pseudo-absences).

World projection of habitat suitability

Only the area between ca. 40°N and ca. 35°S (Fig. 3) had environmental variables within the range used to fit the GLMM. Exceptions occur in some seasons for areas around the west coast of South America and southwest Africa (Fig. 3). In the Atlantic Ocean, highest habitat suitability was patchily distributed in the north (e.g., Gulf of Mexico, Mediterranean Sea, North West coast of Africa) and south (between South America and Africa, but not farther south than 35°S). In the Indian Ocean, areas with highest habitat suitability were mostly near shore; for example: in the Bay of Bengal, Arabian Sea, Mozambique Channel and off Ningaloo Reef (Western Australia). In the western Pacific, highest habitat suitability (albeit lower than in the other oceans) occurred throughout the year (mostly in the central area covered by the tuna purse-seine fisheries).

Projections of future whale shark distribution

The average anomaly forecast for each season in 2070 resulted in an increase of around 0.8–2 °C (Fig. S2) mostly within the region between 30°N and 35°S (commonly considered the whale shark's current latitudinal range; Compagno, 2001). Forecasting suitability based on the 2070 sea surface temperature scenario resulted in a weak but evident pole-ward shift of habitat (Fig. 4 and compare with Fig. 3), mostly in the Atlantic and Indian Oceans. We also observed a general contraction in habitat suitability in 2070 (Table 3 and Fig. 4) with loss of suitable area (in percentage of 9-km grid cells, as
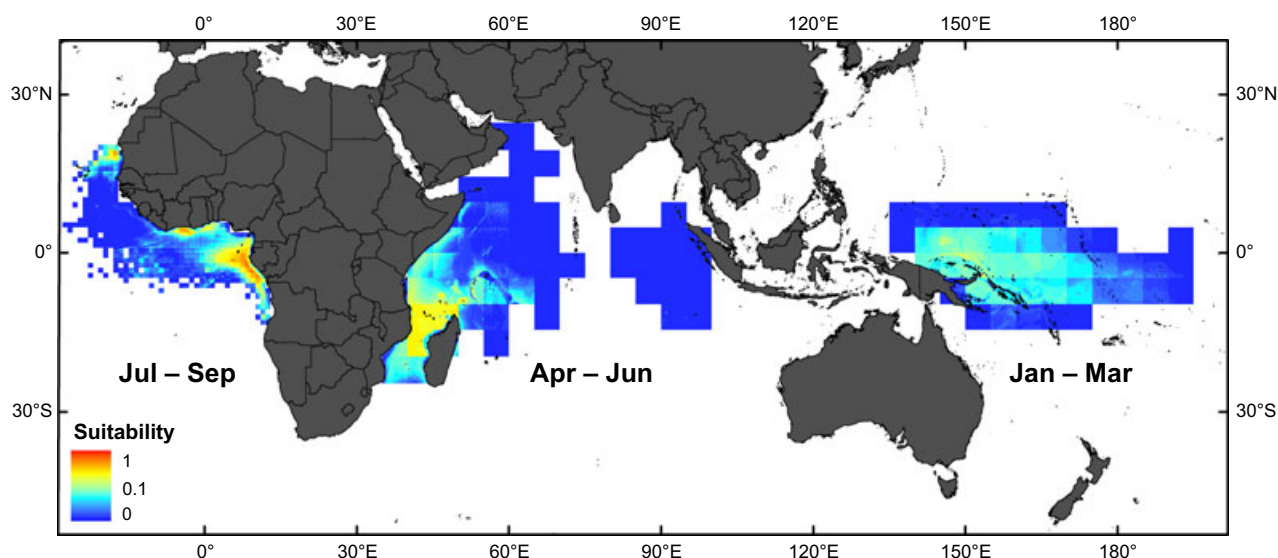

Fig. 2 Predicted whale shark habitat suitability within the area covered by tuna purse-seine fisheries in the peak whale shark occurrence seasons: July–September in the Atlantic, April–June in the Indian and January–March in the western Pacific.
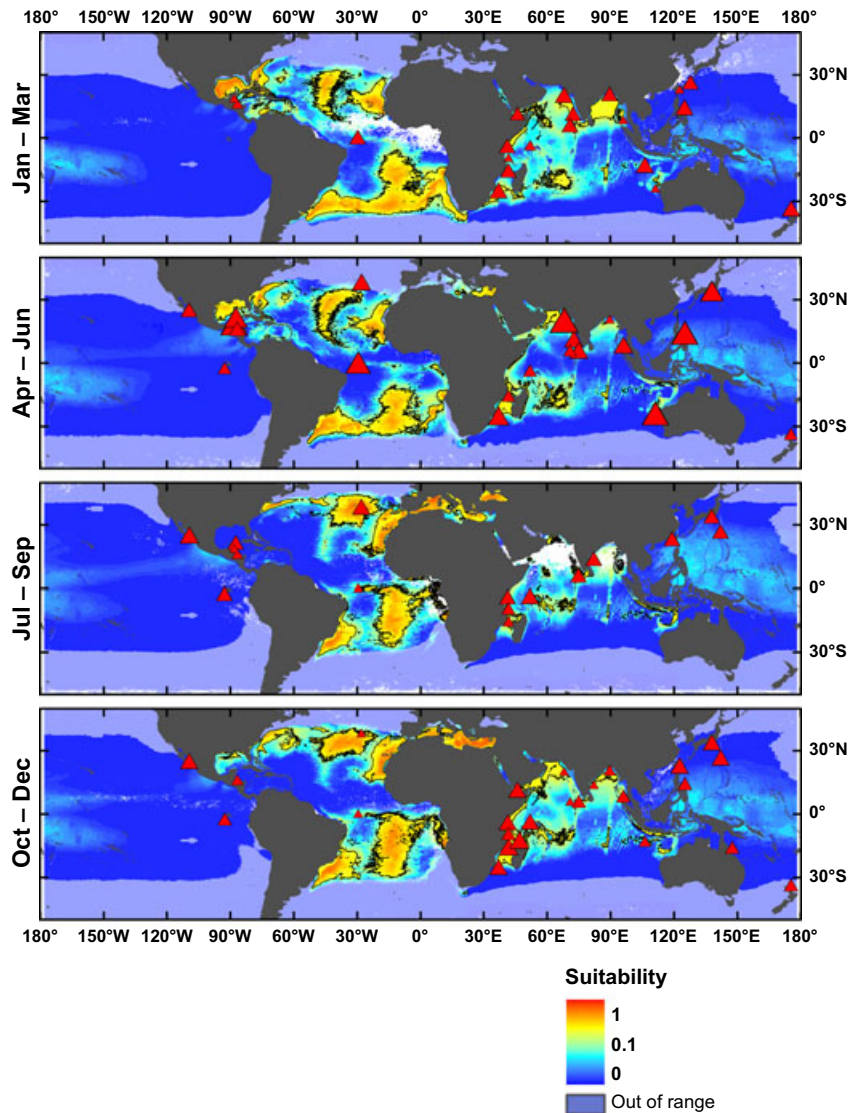
Fig. 3 Global predictions of current seasonal habitat suitability for whale sharks. Prediction maps generated from generalized linear mixed-effects models fit with the sightings and effort data collected by tuna purse-seine fisheries. Where environmental inputs fell outside the environmental space used for the original statistical fit results are shown as 'out of range' in the map. ▲ indicates known aggregation locations within the seasons represented in each map (symbol size proportional to relative size of aggregation). Areas where some environmental predictors were not available (e.g., due to cloud cover) are shown in white (no result). To aid visualization, solid line delineates areas where habitat suitability >0.1 was predicted.

per model resolution) both in the Atlantic and Indian Oceans for most of the year. A maximum loss of ca. 7% was predicted in the Atlantic Ocean for January–March and July–September, and >6% in the Indian Ocean during April–June. The lowest habitat reduction (loss of 2.5% and 3.1% in the Atlantic and Indian Oceans, respectively) was predicted for October–December. Conversely, in the first quarter of the year, our models predicted an expansion of habitat suitability (2.7%) in the Indian Ocean mostly within the Arabian Sea (cf. Figs 3 and 4). In the Pacific, the projected increase in temperature resulted in similar habitat suitability (<0.1

within roughly the same region (no change predicted in percentage of suitable habitat). However, a 'corridor' of suitable habitat linking the western and eastern Pacific Ocean was strengthened for all seasons (Fig. 4).

Discussion

Species distribution models can provide information on suitable habitat for species occurrence (Guisan & Zimmermann, 2000), and coupling them to climate forecasts provides a strong approximation of potential future distributional shifts in response to warming (Hannah
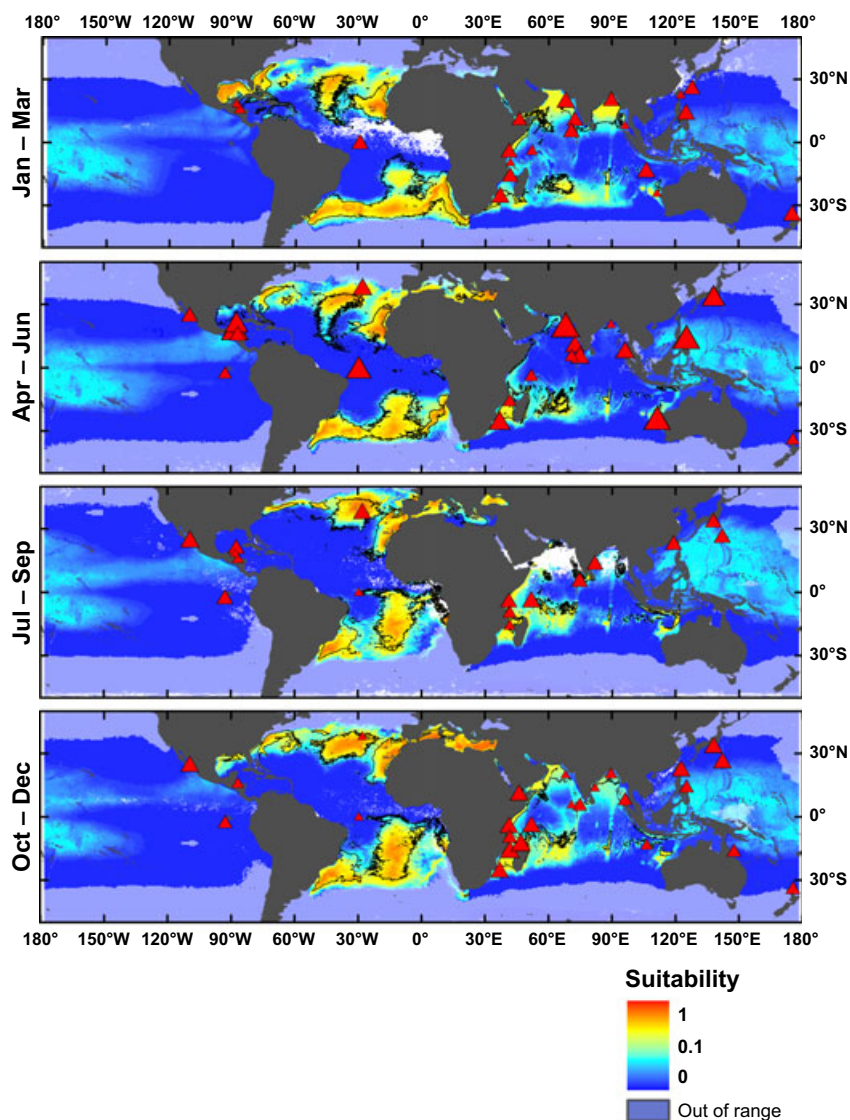
Fig. 4 Predicted shift in global of whale sharks habitat suitability for 2070 under a no-climate-policy reference (no greenhouse gas emissions) reference scenario. Solid line delineates areas where higher habitat suitability (>0.1) had been predicted under current environmental conditions (Fig. 3) for visual assessment of the habitat contraction (reduction in the number of suitable 9-km cells of 5.0% in January–March, 3.3% in April–June, 4.7% in July–September and 6.1% in October–December) and pole-ward shift (ca. 5 °N in January–September in the Atlantic Ocean, and 3–8 °S in the Indian Ocean). ▲ indicates known aggregation locations within the seasons represented in each map, with symbol size proportional to relative size of aggregation (Sequeira *et al.*, 2013b).

Table 3 Predicted change in habitat suitability to 2070. Results are shown in percentage (%) of suitable 9-km grid cells as per model resolution. Arrow direction indicates loss (downward) or gain (upward) of suitable habitat

Ocean	January–March	April–June	July–September	October–December
Atlantic	↓ 7.22	↓ 3.77	↓ 7.35	↓ 2.49
Indian	↑ 2.7	↓ 6.32	↓ 1.08	↓ 3.06
Pacific	no change	no change	no change	no change
Global	↓ 1.4	↓ 2.14	↓ 1.7	↓ 0.97

et al., 2002; Araújo *et al.*, 2005). Such information, reflecting species' susceptibility to anthropogenic climate change, can assist in assessing species-specific vulnerability to changes (Cortés *et al.*, 2010; Gallagher *et al.*, 2012). Access to a global dataset of whale shark sightings provided a unique opportunity to model both current and future habitat suitability over the entire range of this pan-oceanic species. With sea surface temperatures predicted to increase by at least 2 °C on average by 2070 (under a no-climate-policy reference scenario), our GLMM forecast both a (weak) pole-ward shift and contraction of suitable area, with general loss

of habitat (2.5–7.4%) occurring mainly in the warmer equatorial region of the Atlantic and Indian Oceans (Fig. 4). The exception was the Arabian Sea (northwest Indian Ocean) becoming a more suitable area during the first quarter of the year. The general contraction observed is congruent with predictions for zooplankton (Beaugrand *et al.*, 2009), and the general trend (i.e. pole-ward shift) follows predictions for many marine species (Perry *et al.*, 2005; Dulvy *et al.*, 2008). Predicted shifts in habitat suitability are expected in a warming climate because metabolic rates of ectotherms increase with ambient temperature (Makarieva *et al.*, 2005), thereby increasing food-intake requirements and potentially affecting foraging distribution as prey availability shifts. This range shift could be buffered in whale sharks if they modified their diving behaviour to use deeper, cooler waters more frequently as surface water temperatures increase. However, despite the possible oxygen limitations associated with time spent at depth (Graham *et al.*, 2006), prey availability would also be scarce due to their expected shifts (Beaugrand *et al.*, 2009).

The current range of whale sharks is thought to be predominantly between 30°N and 35°S, which generally accords with our current worldwide habitat suitability predictions for the first and last quarters of the year (Fig. 3). However, the environmental envelope predicted during the second and third quarters of the year shifts to latitudes as high as ca. 40°N – a latitude where whale sharks have been reported more recently (e.g., Portugal) (Rodrigues *et al.*, 2012).

Within the Indian Ocean, our current predictions agree with the distribution of observations in that basin (Fig. 3). We predicted high suitability around India, Maldives and Bangladesh, Djibouti, Kenya and Mozambique during the first quarter of the year, (Rowat, 2007; Sequeira *et al.*, 2013b). In the second quarter, we predicted high suitability at Ningaloo Reef (Australia), the Mozambique Channel and Gujarat (India) (Pravin, 2000; Rowat, 2007). From July to September, suitability was highest around the Mozambique Channel (Pierce *et al.*, 2010) and also Seychelles (Rowat, 2007), although we lacked enough data to predict suitability in the northern part of the Indian Ocean. Finally, we predicted high suitability in the last quarter of the year along the east coast of Africa, Bangladesh and Thailand, which also reflects observations (Rowat, 2007).

In the western Pacific, the relatively low habitat suitability is partially a function of the higher sighting (fishing) effort there, which we offset in our models. Regardless, predicted suitability was slightly higher in the Philippines from April to June (Quiros, 2007), and around Taiwan from July to September (Chang *et al.*, 1997) (Fig. 3). In addition, our models suggest the existence of a 'corridor' of suitable habitat, especially between July and September, linking the eastern and western Pacific. This longitudinal pattern was slightly stronger in our scenario for 2070, suggesting its association with warmer temperatures. Our model failed to predict higher suitability in the Gulf of California and the Galapagos where whale sharks occur year round (Cárdenas-Torres *et al.*, 2007) – additional data from the eastern Pacific would probably help improve model performance. However, if habitat in the eastern Pacific remains suitable, this 'corridor' of environmental conditions will possibly permit the connection of whale shark populations across the Pacific. In terrestrial systems where anthropogenic habitat fragmentation is a major threat to biodiversity (Fahrig, 2003), such 'environmentally suitable corridors' are being used to assist species adaptation to climate-driven changes by providing species the opportunity to move to new habitats (Malhi *et al.*, 2008; Vos *et al.*, 2008).

On a worldwide scale, whale shark habitat suitability was highest in the Atlantic Ocean, which is also the region for which the highest-resolution and longest-running data (since 1980) were available. Apart from the Gulf of Mexico and the Azores, there is little other information available for whale sharks in this region to validate qualitatively our model results. In the Azores, occurrences peak at the end of August and September (fisheries data), and in the Gulf of Mexico, they peak in the second quarter of the year (Heyman *et al.*, 2001). These are well predicted in our global model. However, we did not predict high suitability during the following quarter in the Gulf of Mexico where sightings are also known to occur (Motta *et al.*, 2010; De La Parra Venegas *et al.*, 2011). Other suitability congruent with fisheries observations was found in the western coast of Africa mostly between April and September. However, the high suitability predicted in the southern Atlantic cannot yet be validated due to a lack of observations. The high suitability predicted off South Africa in the first quarter of the year is congruent with the hypothesis that whale sharks can cross from the Indian to the Atlantic Ocean through the Cape of Good Hope (Sequeira *et al.*, 2013b). We also predict suitable habitat in the Mediterranean Sea in different quarters of the year (Figs 3 and 4). Despite having water temperatures and being located within the range generally considered suitable for whale sharks (Compagno, 2001), a confirmed sighting has not yet been registered in the area (Psomadakis *et al.*, 2012).

The top-ranked model for all three oceans included the same variables previously identified for the Indian Ocean excluding standard deviation for sea surface temperature (Sequeira *et al.*, 2012, 2013a). However, the interaction terms with ocean resulted in different pre-

dictor importance among oceans. We found evidence that sea surface temperature was an important predictor both in the Atlantic and Indian, but had no discernible effect in the Pacific Ocean. Despite the different sample sizes from each ocean, the range of temperatures for January to March in the Pacific (26.7–30.0 °C) was narrowest when compared to other oceans (25.2–31.2 °C in the Indian, and 19.4–28.3 °C in the Atlantic; Fig. S1), and fell entirely within the range reported for whale shark sightings (26.5–30.0 °C) (Sequeira *et al.*, 2012). *Depth* was an important predictor in the Pacific where the depth range was greater, and in the Atlantic, but not in the Indian Ocean. The relative strength of this predictor among oceans might reflect differences in other depth-associated predictors such as availability of deep-water zooplankton layers available for whale shark feeding (Wilson *et al.*, 2006) not accounted for in our models.

Whale shark occurrence is often associated with productive areas (Taylor & Pearce, 1999), and chlorophyll *a*, a proxy for phytoplankton concentration, has been used successfully to predict occurrence (McKinney *et al.*, 2012). However, we found no evidence that chlorophyll *a* contributed to our global suitability predictions. The broad spatial scale of investigation might contribute to reduce the importance of primary production (cf. Bradshaw *et al.*, 2004), especially in the open ocean where variation in chlorophyll *a* concentration is low. Another explanation might also be associated with possible spatiotemporal lags between primary production and secondary consumers (dilution and downstream effects) (Wafar *et al.*, 1984; Bradshaw *et al.*, 2004), or simply with the need to use weekly averaged values.

To forecast the potential influence of climate change across the circumglobal range of whale sharks (Sequeira *et al.*, 2013b), we derived suitability predictions in areas where predictor values were within the environmental envelope used to calibrate the model (i.e. we only extrapolated our predictions geographically, not environmentally). The correlative approach we used here is sensible for interpolative prediction, while a mechanistic approach is usually more appropriate for extrapolation to novel environments (Kearney & Porter, 2009). To apply the latter approach, however, specific, currently missing data on whale shark life-history traits are required (Sequeira *et al.*, 2013b). Correlative species distribution models, being more flexible in terms of data requirements, were our only option given the available data.

The climate-induced impact on species occurrence is usually investigated by coupling climate forecasts with species distribution models (Hannah *et al.*, 2002; Araújo *et al.*, 2005). However, because this coupling adds extra

limitations, their results provide only a first approximation of possible changes. In the same way, our predictions are intended only to provide a baseline for temperature-dependent forecasts, as we assumed stability of (i) whale shark environmental requirements following niche conservationism (Romdal *et al.*, 2013); and (ii) human disturbances (greenhouse gas emissions are commonly assumed to be stable in climate forecasts). For a more comprehensive study on the influence of temperature in the occurrence of this species, more climate-change scenarios should be tested, and other species distribution models could be generated to assess variability in habitat suitability results, examine error and determine confidence intervals (Thuiller, 2003; Araújo & New, 2006). Likewise, if demographic estimates of vital life history traits become available, they could be integrated into species distribution models to provide direct estimates of future range movement and extinction risk (Fordham *et al.*, 2013a,b). Herein, we focused our species distribution modelling on a hypothesis-testing approach to assess the extent to which the predictors were useful to define suitable whale shark habitat. We therefore used the model-comparison approach only when forecasting changes to sea surface temperature. To improve the predictions derived from our species distribution models, more sightings (ideally with a circumglobal coverage) should also be used. Despite being the largest, most extensive dataset derived from tuna fisheries logbooks, the data we used covered only a portion of areas managed by Regional Fisheries Management Organisations (New Zealand Ministry for Primary Industries http://fs.fish.govt.nz/Page.aspx?pk=103&tk=319). Therefore, there is scope to develop our models based on data from other areas, such as the eastern Pacific Ocean (managed by the Inter-American Tropical Tuna Commission).

The opportunistic dataset we used contained only whale shark presences. We addressed this drawback by randomly generating pseudo-absences (Phillips *et al.*, 2009; Barbet-Massin *et al.*, 2012) and repeating this procedure to account for any biases derived from pseudo-absence selection. However, the dataset used was also only relative to the sea surface, as environmental (and sightings) data spanning subsurface dynamics are not currently available for practical model development, especially where the study area covers most of the global ocean. Furthermore, the dataset included whale shark sightings up to 2010. In recent years, whale sharks have been observed outside the known 30°N–35°S range (Turnbull & Randell, 2006; Rodrigues *et al.*, 2012), so it is possible that our results incorporate an already modified range of suitable habitat.

Despite the current lack of alternatives to fisheries-collected sightings in the open ocean (Jessup, 2003),

combining remotely sensed data with opportunistically recorded occurrences has proven useful for estimating whale shark distributions (McKinney *et al.*, 2012; Sequeira *et al.*, 2012). Indeed, most of our understanding of whale shark ecology and biology hails from opportunistically collected datasets by the ecotourism (e.g., Wilson *et al.*, 2001) or fishing industries near shore at aggregation sites (e.g., McKinney *et al.*, 2012). As such, we should endeavour to analyse all available datasets to provide adequate information for conservation of this pan-oceanic species and largest remaining fish.

Our results demonstrating that global whale shark occurrence is strongly correlated with climatic conditions and that their subpopulations are probably connected globally (Sequeira *et al.*, 2013b) provide a strong incentive for revising current whale shark management policies using a precautionary approach. Unfortunately, existing management is mostly confined to tourist locations, and except for the recent inclusion of this species in the Convention on Migratory Species (CMS, 2010) and the Convention of Trade in Endangered Species (CITES, appendix II; www.cites.org), there are no global measures in place (Rowat & Brooks, 2012). Given that existing management is still regionally focussed and largely fails to take climate change into account, the global conservation of whale sharks is not guaranteed.

References

Araújo MB, New M (2006) Ensemble forecasting of species distributions. *Trends in Ecology and Evolution*, **22**, 42–47.

Araújo MB, Pearson RG, Thuiller W, Erhard M (2005) Validation of species–climate impact models under climate change. *Global Change Biology*, **11**, 1504–1513.

Barbet-Massin M, Jiguet F, Albert CH, Thuiller W (2012) Selecting pseudo-absences for species distribution models: how, where and how many? *Methods in Ecology and Evolution*, **3**, 327–338.

Barve N, Barve V, Jiménez-Valverde A *et al.* (2011) The crucial role of the accessible area in ecological niche modeling and species distribution modeling. *Ecological Modelling*, **222**, 1810–1819.

Beaugrand G, Luczac C, Edwards M (2009) Rapid biogeographical plankton shifts in the North Atlantic Ocean. *Global Change Biology*, **15**, 1790–1803.

Bradshaw CJA, Higgins J, Michael KJ, Wotherspoon SJ, Hindell MA (2004) At-sea distribution of female southern elephant seals relative to variation in ocean surface properties. *ICES Journal of Marine Science*, **61**, 1014–1027.

Bradshaw CJA, Fitzpatrick BM, Steinberg CC, Brook BW, Meekan MG (2008) Decline in whale shark size and abundance at Ningaloo Reef over the past decade: the world's largest fish is getting smaller. *Biological Conservation*, **141**, 1894–1905.

Burnham KP, Anderson DR (2004) Multimodel inference: understanding AIC and BIC in model selection. *Sociological Methods & Research*, **33**, 261–304.

Cárdenas-Torres N, Enríquez-Andrade R, Rodríguez-Dowdell N (2007) Community-based management through ecotourism in Bahia de Los Angeles, Mexico. *Fisheries Research*, **84**, 114–118.

Chang W-B, Ley M-Y, Fang L-S (1997) Embryos of the whale shark, *Rhincodon typus*: early growth and size distribution. *Copeia*, **1997**, 444–446.

Chassot E, Amandè MJ, Chavance P, Pianet R, Dédo Rg RG (2009) Some preliminary results on tuna discards and bycatch in the frend purse seine fishery of the easter Atlantic Ocean. *Collective Volume of Scientific Papers ICCAT*, **64**, 1054–1067.

Clarke LE, Edmonds JA, Jacoby HD, Pitcher H, Reilly JM, Richels R (2007) *Scenarios of greenhouse gas emissions and atmospheric concentrations. A report by the climate change science program and the subcommittee on global change research*, U.S. Climate Change Science Program, Synthesis and Assessment Product 2.1a, Washington, DC.

CMS (2010) Report of the meeting on international cooperation on migratory sharks under the convention on migratory species. *Convention on the Conservation of Migratory Species of Wild Animals*, pp. 1–13. Manila, Philippines. UNEP/CMS/ MS3/REPORT. Available at: www.cms.int/bodies/meetings/regional/sharks/ sharks_meetings.htm (accessed on 30 October 2012).

Cohen J (1960) A coefficient of agreement for nominal scales. *Educational and Psycological Measurement*, **20**, 37–46.

Compagno LJV (2001) *Sharks of the World: An Annotated and Illustrated Catalogue of Shark Species Known to Date, vol. 2: Bullhead, Mackerel and Carpet Sharks (Heterodontiformes, Lamniformes and Orectolobiformes)*, FAO Species Catalogue for Fishery Purposes, Rome.

Cortés E, Arocha F, Beerkircher L *et al.* (2010) Ecological risk assessment of pelagic sharks caught in Atlantic pelagic longline fisheries. *Aquatic Living Resources*, **23**, 25–34.

Davison AC, Hinkley DV (1997) *Bootstrap Methods and Their Application*. Cambridge University Press, New York, USA.

De La Parra Venegas R, Hueter R, Cano JG *et al.* (2011) An unprecedented aggregation of whale sharks, *Rhincodon typus*, in Mexican coastal waters of the Caribbean Sea. *PLoS ONE*, **6**,e18994, doi:18910.11371/journal.pone.0018994.

Dulvy NK, Rogers SI, Jennings S, Stelzenmüller V, Dye SR, Skjoldal HR (2008) Climate change and deepening of the North Sea fish assemblage: a biotic indicator of warming seas. *Journal of Applied Ecology*, **45**, 1029–1039.

Edwards M, Richardson AJ (2004) Impact of climate change on marine pelagic phenology and trophic mismatch. *Nature*, **430**, 881–884.

Elith J, Leathwick JR (2009) Species distribution models: ecological explanation and prediction across space and time. *Annual Review of Ecology, Evolution and Systematics*, **40**, 677–697.

Fahrig L (2003) Effects of habitat fragmentation on biodiversity. *Annual Review of Ecology, Evolution, and Systematics*, **34**, 487–515.

Fordham DA, Wigley TML, Brook BW (2011) Multi-model climate projections for biodiversity risk assessments. *Ecological Applications*, **21**, 3317–3331.

Fordham DA, Wigley TML, Watts MJ, Brook BW (2012) Strengthening forecasts of climate change impacts with multi-model ensemble averaged projections using MAGICC/SCENGEN 5.3. *Ecography*, **35**, 4–8.

Fordham DA, Akçakaya HR, Araújo MB, Keith DA, Brook BW (2013a) Tools for integrating range change, extinction risk and climate change information into conservation management. *Ecography*, **36**, 956–964. doi:10.1111/j.1600-0587.2013. 00147.x.

Fordham DA, Brook BW, Caley MJ, Bradshaw CJA, Mellin C (2013b) Conservation management and sustainable harvest quotas are sensitive to choice of climate modelling approach for two marine gastropods. *Diversity and Distributions*, doi:10. 1111/ddi.12092.

Gallagher AJ, Kyne PM, Hammerschlag N (2012) Ecological risk assessment and its application to elasmobranch conservation and management. *Journal of Fish Biology*, **80**, 1727–1748.

GeBCO (2003) *General Bathymetric Chart of the Oceans - One Minute Gridversion, 2.0*. Available at: http://www.gebco.net (accessed on 16 June 2009).

Graham RT, Roberts CM, Smart JCR (2006) Diving behaviour of whale sharks in relation to a predictable food pulse. *Journal of the Royal Society*, **3**, 109–116.

Guisan A, Zimmermann NE (2000) Predictive habitat distribution models in ecology. *Ecological Modelling*, **135**, 147–186.

Gutierrez AP, Ponti L, D'oultremont T, Ellis CK (2008) Climate change effects on poikilotherm tritrophic interactions. *Climatic change*, **97** (Suppl. 1), S167–S192.

Hannah L, Midgley GF, Millar D (2002) Climate change-integrated conservation strategies. *Global Ecology and Biogeography*, **11**, 485–495.

Heyman WD, Graham RT, Kjerfve B, Johannes RE (2001) Whale sharks *Rhincodon typus* aggregate to feed on fish spawn in Belize. *Marine Ecology Progress Series*, **215**, 275–282.

Heyman WD, Carr LM, Lobel PS (2010) Diver ecotourism and disturbance to reef fish spawning aggregations: it is better to be disturbed than to be dead. *Marine Ecology Progress Series*, **419**, 201–210.

Jessup D (2003) Opportunistic research and sampling combined with fish and wildlife management actions or crisis response. *Institute for Laboratory Animal Research*, **44**, 277–285.

Kearney M, Porter W (2009) Mechanistic niche modelling: combining physiological and spatial data to predict species ranges. *Ecology Letters*, **12**, 334–350.

Makarieva AM, Gorshkov VG, Li B-L (2005) Temperature-associated upper limits to body size in terrestrial poikilotherms. *Oikos*, **111**, 425–436.

Malhi Y, Roberts JT, Betts RA, Killeen TJ, Li W, Nobre CA (2008) Climate change, deforestation, and the fate of the Amazon. *Science*, **319**, 169–172.

McKinney JA, Hoffmayer ER, Wu W, Fulford R, Hendon JM (2012) Feeding habitat of the whale shark *Rhincodon typus* in the northern Gulf of Mexico determined using species distribution modelling. *Marine Ecology Progress Series*, **458**, 199–211.

Mellin C, Huchery C, Caley MJ, Meekan MG, Bradshaw CJA (2010) Reef size and isolation determine the temporal stability of coral reef fish populations. *Ecology*, **91**, 3138–3145.

Motta PJ, Maslanka M, Hueter RE *et al.* (2010) Feeding anatomy, filter-feeding rate, and diet of whale sharks *Rhincodon typus* during surface ram filter feeding off the Yucatan Peninsula, Mexico. *Zoology*, **113**, 190–212.

Parmesan C (2006) Ecological and evolutionary responses to recent climate change. *Annual Review of Ecology, Evolution and Systematics*, **37**, 637–669.

Perry AL, Low PJ, Ellis JR, Reynolds JD (2005) Climate change and distribution shifts in marine fishes. *Science*, **308**, 1912–1915.

Phillips SJ, Dudík M, Elith J, Graham CH, Lehmann A, Leathwick J, Ferrier S (2009) Sample selection bias and presence-only distribution models: implications for background and pseudo-absence data. *Ecological Applications*, **19**, 181–197.

Pierce SJ, Méndez-Jiménez A, Collins K, Rosero-Caicedo R, Monadjem A (2010) Developing a code of conduct for whale shark interactions in Mozambique. *Aquatic Conservation: Marine and Freshwater Ecosystems*, **20**, 782–788.

Praca E, Gannier A (2007) Ecological niche of three teuthophageous odontocetes in the northwestern Mediterranean Sea. *Ocean Science Discussions*, **4**, 785–815.

Pravin P (2000) Whale shark in the Indian coast – need for conservation. *Current science*, **79**, 310–315.

Psomadakis PN, Giustino S, Vacchi M (2012) Mediterranean fish biodiversity: an updated inventory with focus on the Ligurian and Tyrrhenian seas. *Zootaxa*, **3263**, 1–46.

Quiros AL (2007) Tourist compliance to a code of conduct and the resulting effects on whale shark (*Rhincodon typus*) behavior in Donsol, Philippines. *Fisheries Research*, **84**, 102–108.

R Development Core Team (2012) *R: A Language and Environment for Statistical Computing*. R Foundation for Statistical Computing. ISBN 3-900051-07-0, Vienna, Austria. Available at: http://www.R-project.org/ (accessed on July 2012).

Reichler T, Kim J (2008) How well do coupled models simulate today's climate? *Bulletin of the American Meteorological Society*, **89**, 303–311.

Richardson AJ, Poloczanska ES (2008) Under-resourced, under threat. *Science*, **320**, 1294–1295.

Riley MJ, Harman A, Rees RG (2009) Evidence of continued hunting of whale sharks *Rhincodon typus* in the Maldives. *Environmental Biology of Fishes*, **86**, 371–374.

Rodrigues NV, Correia JPS, Graça JTC, Rodrigues F, Pinho R, Hirofumi M (2012) First record of a whale shark *Rhincodon typus* in continental Europe. *Journal of Fish Biology*, doi:10.1111/j.1095-8649.2012.03392.x.

Romdal TS, Araújo MB, Rahbek C (2013) Life on a tropical planet: niche conservatism and the global diversity gradient. *Global Ecology and Biogeography*, **22**, 344–350.

Rowat D (2007) Occurrence of whale shark (*Rhincodon typus*) in the Indian Ocean: a case for regional conservation. *Fisheries Research*, **84**, 96–101.

Rowat D, Brooks KS (2012) A review of the biology, fisheries and conservation of the whale shark *Rhincodon typus*. *Journal of Fish Biology*, **80**, 1019–1056.

Sequeira A, Mellin C, Rowat D, Meekan MG, Bradshaw CJA (2012) Ocean-scale prediction of whale shark distribution. *Diversity and Distributions*, **18**, 504–518.

Sequeira A, Mellin C, Delean S, Meekan MG, Bradshaw CJA (2013a) Spatial and temporal predictions of decadal trends in Indian Ocean whale sharks. *Marine Ecology Progress Series*, **478**, 185–195.

Sequeira AMM, Mellin C, Meekan MG, Sims DW, Bradshaw CJA (2013b) Inferred global connectivity of whale shark *Rhincodon typus* populations. *Journal of Fish Biology*, **82**, 367–389.

Sleeman JC, Meekan MG, Wilson SG *et al.* (2007) Biophysical correlates of relative abundances of marine megafauna at Ningaloo Reef, Western Australia. *Marine and Freshwater Research*, **58**, 608–623.

Speed CW, Meekan MG, Rowat D, Pierce SJ, Marshall AD, Bradshaw CJA (2008) Scarring patterns and relative mortality rates of Indian Ocean whale sharks. *Journal of Fish Biology*, **72**, 1488–1503.

Taylor KE (2001) Summarizing multiple aspects of model performance in a single diagram. *Journal of Geophysical Research*, **106**, 7183–7192.

Taylor JG, Pearce AF (1999) Ningaloo Reef currents: implications for coral spawn dispersal, zooplankton and whale shark abundance. *Journal of the Royal Society of Western Australia*, **82**, 57–65.

Thomas CD, Cameron A, Green RE *et al.* (2004) Extinction risk from climate change. *Nature*, **427**, 145–148.

Thuiller W (2003) BIOMOD – optimizing predictions of species distributions and projecting potential future shifts under global change. *Global Change Biology*, **9**, 1353–1362.

Thums M, Meekan M, Stevens J, Wilson S, Polovina J (2012) Evidence for behavioural thermoregulation by the world's largest fish. *Journal of the Royal Society Interface*, **10**, doi:10.1098/rsif.2012.0477.

Tittensor DP, Mora C, Jetz W, Lotze HK, Ricard D, Berghe EV, Worm B (2010) Global patterns and predictors of marine biodiversity across taxa. *Nature*, **466**, 1098–1104.

Turnbull SD, Randell JE (2006) Rare occurrence of a *Rhincodon typus* (Whale shark) in the Bay of Fundy, Canada. *Northeastern Naturalist*, **13**, 57–58.

Vos CC, Berry P, Opdam P *et al.* (2008) Adapting landscapes to climate change: examples of climate-proof ecosystem networks and priority adaptation zones. *Journal of Applied Ecology*, **45**, 1722–1731.

Wafar M, Le Corre P, Birrien J-L (1984) Seasonal changes of dissolved organic matter (C, N, P) in permanently well mixed temperate waters. *Limnology and Oceanograohy*, **29**, 1127–1132.

Wernberg T, Russell BD, Thomsen MS, Gurgel CFD, Bradshaw CJA, Poloczanska ES, Connell SD (2011) Seaweed communities in retreat from ocean warming. *Current Biology*, **21**, 1828–1832.

Wilson SG, Taylor JG, Pearce AF (2001) The seasonal aggregation of whale sharks at Ningaloo Reef, Western Australia: currents, migrations and the El Niño/Southern Oscillation. *Environmental Biology of Fishes*, **61**, 1–11.

Wilson SG, Polovina JJ, Stewart BS, Meekan MG (2006) Movements of whale sharks (*Rhincodon typus*) tagged at Ningaloo Reef, Western Australia. *Marine Biology*, **148**, 1157–1166.

Supporting Information

Additional Supporting Information may be found in the online version of this article:

Figure S1. Boxplots for major environmental predictors within the area covered by the fisheries in each ocean. Upper and lower limits indicate the maximum and minimum values in each dataset.

Figure S2. Global sea surface temperature averages from April to June. Top panel: current temperatures as seasonal averages for 2002–2012 derived from MODIS-Aqua satellite. Bottom panel: increase in sea surface temperatures predicted by 2070. The climate change scenario for 2070 was obtained by adding the predicted increase calculated by an ensemble forecast of climate change derived from five global circulation models: CCSM-3, MRI-CGCM2.3.2, ECHAM5/MPI-OM, MIROC3.2 (hires) and UKMO-HadCM3. These GCM were chosen based on their global skill in predicting recent SST temperatures (1981–2000). Model terminology follows CMIP3 Multi-Model Dataset Archive naming convention (www-pcmdi.llnl.gov/ipcc/about_ipcc.php), and baseline observed temperatures used were from 1995 (AV-HRR Pathfinder).